Published in: Materials Chemistry & Physics (2009), vol.116, iss.2-3, pp.368-375
Status: Postprint (Author's version)

Interactions in $YBa_2Cu_3O_{7-x}$ aqueous suspensions

Laurent Dusoulier[a,b], Rudi Cloots[a], Bénédicte Vertruyen[a], Jose L. Garcia-Fierro[c], Rodrigo Moreno[d], Begoña Ferrari[d]

[a] *SUPRATECS, Institut de chimie B6a, Université de Liège, B-4000, Liège, Belgium*
[b] *Royal Military Academy, CISS Department, Brussels, Belgium*
[c] *Institute de Catálisis y Petroquímica, CSIC, Campus de Cantoblanco, c/Marie Curie 2, 28049, Madrid, Spain*
[d] *Institute de Cerámica y Vidrio, CSIC, Campus de Cantoblanco, c/Kelsen 5, 28049, Madrid, Spain*

Abstract: Surface charging mechanism of $YBa_2Cu_3O_{7-x}$ (YBCO) particles in water has been investigated in order to understand their colloidal behaviour and stabilise concentrated suspensions. A broad study relating the suspension parameters (pH and zeta potential) vs. the conditions of the suspension performance (atmosphere and time) has been shown and discussed. The zeta potential values remain positive in all the pH range for the highest powder concentration studied (10 gl^{-1}), evidencing a large influence of the solid content in the particle charge. The chemistry of $YBa_2Cu_3O_{7-x}$ in water has been studied through the chemical analysis of the supernatant by inductively coupled plasma (ICP), and the surface analysis of the particles by X-ray diffraction analysis (XRD) and X-ray photoelectron spectroscopy (XPS). The presence of $BaCO_3$, CuO, and the hydrolysed Ba species, such as $Ba(OH)_2$ and $Ba(OH)^+$, at the particles surface has been evaluated as a function of the powder concentration. Based on these analyses, the dependence of the colloidal behaviour of YBCO on the presence of Ba soluble species has been determined. A stabilisation mechanism for YBCO particles in aqueous suspension focus on the powders deleterious minimization was proposed.

Keywords: Ceramics; Surfaces; Superconductors; X-ray photo-emission spectroscopy (XPS)

1. Introduction

Metal oxides cover one of the widest groups of materials with important structure-related properties. Metal oxides can exhibit ferroelectricity, magnetism, superconductivity, colossal magnetoresistivity, photoluminescence, conductivity, gas-sensing capabilities, etc., evidencing that their processing will lead to key development in device performance. Many of these inorganic materials are binary or ternary oxides, i.e. titanates ($ATiO_3$ or $A_2Ti_nO_{2n+1}$, where A = alkaline earth or alkali metal), multiferroics ($RMnO_3$ where R=Sc, Y, In, Bi, Er,...), second generation superconductors ($REBa_2Cu_3O_7$, where RE = rare earth metal) or ABO_4-type structures (A and B are elements with oxidation states of 2+ and 6+), etc. The cations activity determines the reliability and the reproducibility of manufactured structures of these compounds. Otherwise, the relation between structure and properties has reached new perspectives with the developments of nanostructured materials, in which the interaction of the surfaces with the surrounding media has a special relevance.

The processing into highly textured forms is a major problem of binary and ternary oxides. Vacuum processes, such as liquid-phase epitaxy (LPE) or physical vapour deposition (PVD), etc., produce high quality materials but have problems related to scaling-up and cost. Alternative low-cost and non-vacuum processes are receiving considerable interest, specially liquid-phase synthesis (sol-gel, co-precipitation, hydrothermal synthesis) combined with coating technologies (spraying, dipping, tape casting or electrophoretic deposition). The success of the processes developed in liquid media depends on the surface chemistry of the powders, which determines the properties of the coatings, but also the preparation of stable suspensions is essential to produce homogeneous materials with improved reliability [1-3]. Hence, an exhaustive study of the colloidal behaviour is necessary to assure reliable properties.

Since the discovery of high temperature superconductors (HTS) by Bednorz and Müller in 1986, considerable research effort has been devoted to the study and improvement of the superconducting properties of such materials. For most practical applications, a high current density (J_c) is required. $YBa_2Cu_3O_{7-x}$ (YBCO) is the current material choice for second generation superconducting wires or films, which new processing strategies and low-cost production have been investigated [4-7]. However, fundamental and practical problems have to be still solved. $YBa_2Cu_3O_{7-x}$ has demonstrated its instability in different environmental conditions: humid atmosphere, water, acids, alkalis, etc. [8-13]. It is well known that a slow irreversible chemical decomposition under ambient atmospheric conditions leads to degradation of superconducting material into non-superconducting phases following Eq. (1):

$$YBa_2Cu_3O_{7-x} + 1.5H_2O \rightarrow 2.5CuO + 1.5Ba^{2+} + 3OH^- + 0.5Y_2BaCuO_5 + 0.25O_2 \quad (1)$$

Several reports [8-13] have demonstrated that YBCO powders in aqueous medium undergo Ba^{2+} leaching and pH increases, as reported for other compounds like $BaTiO_3$ [14-18] and $BaZrO_3$ [19]. Also, a strong decomposition of YBCO occurs under very acidic conditions, and green Y_2BaCuO_5 (Y-211) phase appears [8-10], discouraging the colloidal processing of these powders at pH below 6. However, the colloidal behaviour of YBCO suspensions prepared under basic conditions, and the properties related consequences, has not been characterised in depth.

Humid atmosphere is a common environment in the operating conditions of HTS and has a detrimental effect on the properties of the material [20,21]. To date, very few studies concerning the colloidal stability of YBCO particles either in water or in organic media have been reported and available data dealing with zeta potential measurements and the determination of the isoelectric point (IEP) are scarce [22,23]. The study of the charging mechanism and the surface chemistry of YBCO in water is a basic step to understand its colloidal behaviour, in order to allow manufacturing dense films with uniform microstructures.

In this work, the stability and surface charging mechanism of YBCO particles in water has been investigated in terms of powder dissolution and zeta potential, as a function of pH, solid content and suspension performance conditions (atmosphere and time).

Table 1: *Concentrations of the elements dissolved in the supernatants of 0.1,1 and 10 gl^{-1} suspensions related to the initial pH and the pH measured in equilibrium. Concentrations of the elements dissolved in the supernatants of 10gl^{-1} suspensions prepared at a prefixed pH of 10.1,6.7 and 4.7.*

Concentration (gl^{-1})	Initial pH	pH in equilibrium	$[Cu(II)_{aq}]$(mmol l^{-1})	$[Y(III)_{aq}]$(mmol l^{-1})	$[Ba(II)_{aq}]$(mmol l^{-1})
0.1	7.5	7.3	<0.02	<0.01	0.04
1	10.5	8.0	<0.02	<0.01	0.23
10	12.0	12.5	<0.02	<0.01	21.85
10	-	10.1	<0.02	<0.01	9.30
10	-	6.7	1.3	<0.01	3.30
10	-	4.7	7.9	15.7	29.10

2. Materials and methods

2.1. Powder characterisation

As starting material a commercial 99.9% purity $YBa_2Cu_3O_{7-x}$ (YBCO) powder from Alfa-Aesar (Germany) was used. This compound was synthesised by the spray-pyrolysis technique. This powder has mean particle size of 4 μm, specific surface area of 1.4 m^2 g^{-1} and density of 5.91 g cm^{-3}. The particle size distribution was determined with a laser diffraction particle size analyser (Mastersizer S, Malvern, UK), the surface areas by single point N_2 adsorption (BET Monosorb, Quantachrome, USA), and the density with a He-multipicnometer (Qjiantachrome, USA). No pre-treatments were realised on the powder for suspension preparation. For comparison purposes, a $BaCO_3$ powder supplied by Alfa-Aesar (Germany) was also used for its IEP determination.

2.2. Experimental techniques

Suspensions were prepared to solid concentrations of 0.1, 1 and 10gl^{-1}, by adding the appropriate amount of YBCO powder in deionised water using polyethylene containers. Dispersion was achieved by sonication (US) using a 400W probe (IKA U400S, Germany) for 1.5 min and further stirring.

The surface behaviour of YBCO in water was determined in terms of pH and zeta potential as a function of the homogenisation time, using air and nitrogen (N_2) atmosphere. Suspensions were prepared at 0.1, 1 and 10gl^{-1} solid loadings. Experiments were also carried out reducing the presence of CO_2 by using water boiled for 1 h and maintaining a constant nitrogen flow in the measurement cell.

Zeta potential measurements were performed by laser Doppler velocimetry (Zetasizer NanoZS, Malvern, UK), using the Smoluchowski equation to calculate the zeta potential from mobility data. Three measurements for each sample were made being the standard deviation ±5 mV. The IEP of YBCO suspensions was determined at a fixed ionic strength using 10^{-2} M KCl solutions as electrolyte. Adjustments of pH were performed by adding small amounts of HCl or KOH 10^{-1} M controlled by a standard glass electrode pH-meter. Zeta potential was then measured in equilibrium, from suspensions maintained under constant stirring during 48 h. The IEP of 0.1 gl^{-1} $BaCO_3$ suspensions was also determined. The $BaCO_3$ suspensions were prepared following the same procedure used for YBCO powders.

Nitrate salts of Y, Ba and Cu ($Y(NO_3)_3$ $6H_2O$,99.9% purity; $Ba(NO_3)_2$,99% purity; and $Cu(NO_3)_2$ $3H_2O$, 98% purity) supplied by Alfa-Aesar (Germany) were used to check the adsorption of cations in dilute aqueous suspensions (0.1 g l^{-1}). Ba^{2+} ions were also added varying the suspension pH. After each salt addition, suspensions were maintained under stirring for 15 min and zeta potentials were subsequently measured.

Chemical analysis was performed by inductively coupled plasma-atomic emission spectroscopy (ICP-AES, Thermo Jarrell Ash, Iris Advantage Duo, USA) on the supernatant obtained after filtration and centrifugation (3500 rpm, 2 x 10 min) of settled suspensions. The powders obtained from suspensions prepared at different pH and solid loadings were characterized by X-ray diffraction analysis (XRD) using Cu Kα radiation (Siemens D5000, Germany) and by X-ray photoelectron spectroscopy (XPS). Photoelectron spectra were obtained using a Fisons Escalab 200R spectrometer using Mg Kα X-ray (photon energy, hv= 1253.6 eV) source. The sample was first placed in an aluminum holder fixed on a sample-rod in the pretreatment chamber of the spectrometer and then degassed at room temperature for 1 h before being transferred to the analysis chamber. All the spectra were recorded in the constant pass energy mode (20 eV). A survey spectrum was recorded for each sample (single scan) followed by detailed analysis (60 scans) of Cu $2p_{3/2}$, Ba $3d_{5/2}$, Y $3d_5/_2$, and O 1s energy regions. The binding energies (BEs) were referenced to the spurious C 1s peak (284.6 eV) used as internal standard to take into account charging effects. The accuracy of quantitative analysis is about 4% and the precision in the BE is estimated to be ±0.1 eV. The areas of the peaks were computed by fitting the experimental spectra to Gaussian/Lorentzian curves after removal of the background (Shirley function). Surface atom ratios were calculated from peak area ratios normalized by the corresponding atomic sensitivity factors [24].

3. Results and discussion

3.1. Surface chemistry of YBCO particles in aqueous suspensions

In order to determine the extent of YBCO dissolution in aqueous suspensions, chemical analysis was performed by ICP using suspensions submitted to surface equilibrium in air. ICP analysis was performed for 0.1, 1 and 10g l^{-1} suspensions. Element concentrations were determined for the supernatants obtained after centrifugation of suspensions dispersed by US and homogenised during 48 h. The suspensions concentration, their initial pH, the pH achieved in equilibrium (after 48 h stirring) and the ICP results, are listed in Table 1. A similar analysis was done for concentrated suspensions (10g l^{-1}) prepared at a prefixed pH value of 10.1, 6.7 and 4.7, and the results are also shown in Table 1. The pH values measured during the homogenisation time will be the denominated natural pH, opposed to the pH prefixed adding KOH and HCl.

Related to the variation in solid loading of the YBCO suspensions, the concentrations of $Y(III)_{aq}$ and $Cu(II)_{aq}$ are negligible (<0.01 and 0.02 mmol l^{-1}, respectively) compared to that of $Ba(II)_{aq}$, especially at the highest solid content. According to other authors [8,10] an incongruent dissolution occurs in YBCO aqueous suspensions because a significant fraction of Ba^{2+} is leached from the surface without effect on $Y(III)_{aq}$ and $Cu(II)_{aq}$ concentrations. The solid content also determines the natural pH of the suspension after US and in equilibrium, evidencing the development of different chemical reactions. The natural pH of 0.1, 1 and 10gl^{-1} suspensions in equilibrium are 7.3, 8.0 and 12.5, respectively.

Fig. 1: *Concentration/pH diagram of (a) $Cu(II)_{aq}$ and (b) $Ba(II)_{aq}$.*

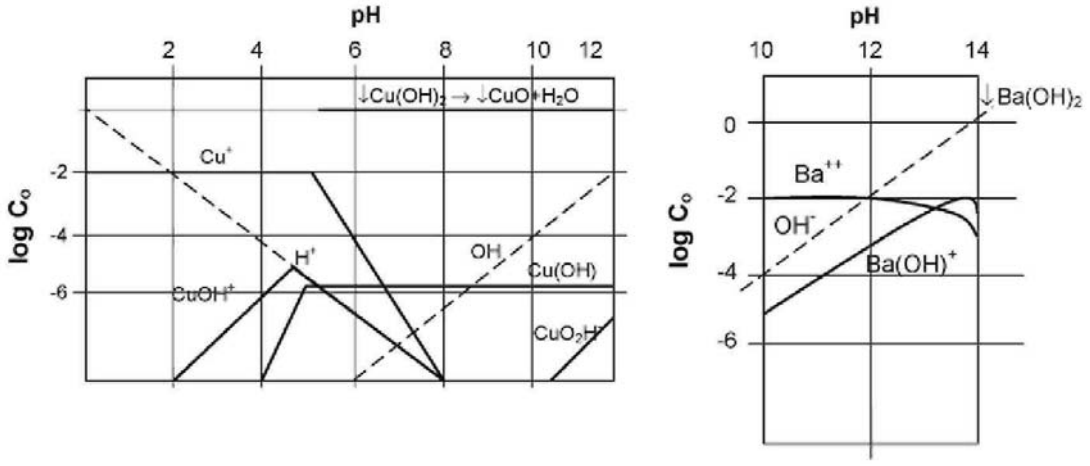

A high concentration of $Ba(II)_{aq}$ was measured for 10gl^{-1} suspensions (21.85 mmol l^{-1}). Otherwise, when concentrated suspensions were prepared at a prefixed pH, the concentration of soluble species of Ba decreases to 9.30mmol l^{-1} at pH 10.1, and 3.30 mmol l^{-1} at pH 6.7. The $Cu(II)_{aq}$ and $Y(III)_{aq}$ concentrations maintain below the detection limit of the ICP analysis at pH 10.1, although a small amount of $Cu(II)_{aq}$ can be measured (1.30 mmol l^{-1}) at pH 6.7. Finally, high concentrations of $Ba(II)_{aq}$, $Y(III)_{aq}$ and $Cu(II)_{aq}$ are detected in the supernatant for acidic pH (~5), as expected due to powder decomposition [8-10].

The logC/pH equilibrium diagrams for $Cu(II)_{aq}$ and $Ba(II)_{aq}$ [25] are shown in Fig. 1 a and b, respectively. Cu^{2+} ions are identified as the predominant species at acidic pH in Fig. la. Precipitation of $Cu(OH)_2$ occurs above pH 5, which evolves to the oxide formation (CuO). Otherwise, the equilibrium diagram of $Ba(II)_{aq}$ (Fig. 1b) shows that $Ba(OH)_2$ precipitates at a very basic pH, suggesting that part of the leached Ba^{2+} from the YBCO surface becomes $Ba(OH)^+$ over pH 10. The high concentration of $Ba(II)_{aq}$ determined by ICP in the supernatant of the 10g l^{-1} suspensions (>0.1 mmol l^{-1}) at pH > 10 suggests that $Ba(OH)^+$ coexists with Ba^{2+} in solution under basic conditions.

To determine the phases formed in 10g l^{-1} YBCO suspensions in water, XRD analysis was performed on dry powders, previously suspended at different pH conditions and maintained stirring for 12 and/or 48 h (Fig. 2). The absence of a representative amount of the Y-211 phase is noticed in all cases [26]. The presence of $BaCO_3$ and CuO are observed after 48 h at the natural pH of the suspension (pH 12). $BaCO_3$ can be also slightly detected at this pH (~12) after 12 h stirring. However, when suspensions were prepared at a prefixed pH (10, 7.8 and 6.8), the CuO and $BaCO_3$ diffraction peaks cannot be identified.

The XRD patterns suggest the formation of $BaCO_3$ and CuO during the homogenisation time. If we consider the distribution function of CO_3^{2-} in solution, the major species at basic pH is CO_3^{2-}as the formation of $BaCO_3$ is higher than under acid conditions. Otherwise, Eq. (1) also determines the formation of CuO as a product of the YBCO dissolution.

However, the formation of these species have been partially inhibited when the pH was prefixed in a range of 7≤pH≤10, being their concentrations lower than the XRD detection limit (5 wt.%). The log C/pH equilibrium diagram of $Cu(II)_{aq}$ determines the increase of Cu solubility at pH<8. In fact, the results of the ICP analysis summarised in Table 1 reveal an increase of the Cu solubility for pH 6.7, which could be related with the absence of the CuO spectra in XRD patterns for 10g l^{-1} suspensions prepared at pH<8. However, CuO is not detected either at pH 10. Otherwise, the ICP results shown in Table 1 demonstrate that the Ba solubility decreases when imposed pH tends toward neutral values. Both facts, the absence of $BaCO_3$ and CuO patterns in the XRD spectra and the decrease of Ba solubility, suggest a lower YBCO dissolution when the pH was prefixed within the range 7<pH< 10 at the concentrated suspensions (Table 1 and Fig. 2).

The YBCO particles were also analysed by XPS after being filtrated and dried. The powders analysed in this case are the as-received powders and those coming from suspensions prepared at the three different concentrations (0.1,1 and 10g l^{-1}) at their pH in equilibrium (7.3, 8.0, and 12.5, respectively). In XPS spectra, the Cu 2p line profile shows in all cases the characteristic spin-orbit doublet together with the satellite lines placed at the high BE side (ca. 9 eV) of the principal peaks, which is the fingerprint of Cu^{2+} ions. Similarly, the BE of Y

$3d_{5/2}$ and Ba $3d_{5/2}$ peaks are typical of Y^{3+} and Ba^{2+} ions. Ba 3d peaks of representative samples are plotted in Fig. 3. All BE and peaks percentages are summarised in Table 2.

C 1s profiles are complex because one or two components in the region 288.3-290.3 eV, in addition to adventitious carbon, were found. The high energy signal of the O1s (532.8 eV) and the C 1s (289.2 eV) spectra have been related to the presence of carbonated/oxycarbonated species [27]. Then, the XPS spectra verify the presence of a contaminated surface even in the as-received YBCO powders [27,28]. In fact, the lowest BE contribution of O 1s spectra (529.4 eV) and the Cu $2p_{3/2}$ peak at 933.8 eV has been also associated to the presence of CuO [27,29]. The O 1s peak at ~531.0 eV, besides to identify the characteristic YBCO feature according to the Y $3d_{5/2}$ peak observed at 157.5 eV [29], is in the range of reported values for Ba hydrolysed species ($Ba(OH)_2$ and $Ba(OH)^+$) considering the Ba $3d_{5/2}$ at 779.8 eV [27]. Hence, XPS spectra suggest the presence of $Ba(OH)^+$, $Ba(OH)_2$, $BaCO_3$ and CuO at the surface of the starting powder and after dispersion in water, in good agreement with the XRD and ICP results discussed above.

Fig. 2: *XRD patterns of YBCO powders obtained for 10g l^{-1} suspensions prepared under different pH conditions, and stirred for 12 h (pH 6.8, 7.8,10 and 12) and 48 h (pH 12).*

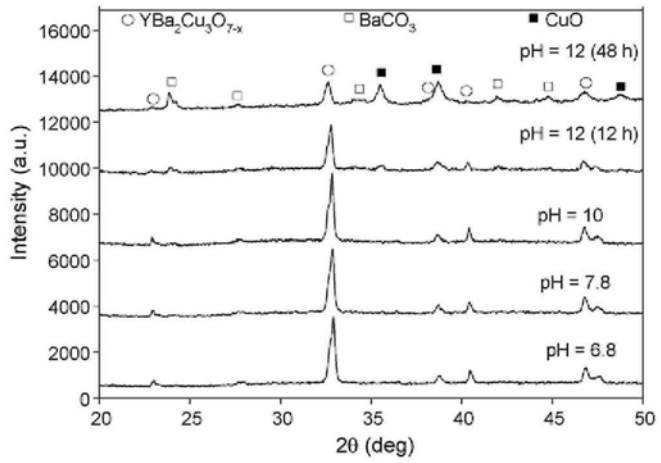

Table 2: *BE (eV) of core-levels of YBaCuO samples vs. the suspension concentration (numbers in parentheses are peak percentages).*

Sample	Cu $2p_{3/2}$	Ba $3d_{5/2}$	Y$3d_{5/2}$	O 1s	C 1s
	933.8	779.8	157.4	529.4 (23)	284.9 (26)
As-received				530.9(61)	
				532.8 (16)	289.2 (74)
	933.7	780.2	157.4	529.4 (26)	284.9 (56)
0.1gl^{-1}\pH7.3				531.2(50)	
				532.9 (24)	289.4 (44)
	933.9	780.3	157.7	529.3 (22)	284.9 (40)
lg1^{-1},pH8.0				531.1 (53)	288.3 (24)
				532.7 (23)	290.0 (36)
	933.5	780.6	157.6	529.4 (50)	284.9 (49)
10gl^{-1},pH 12.5				531.0(31)	288.8(22)
				532.9(19)	290.5 (29)

According to the assignment of the XPS peaks, the variation of the peaks percentages could help to determine the general state of the particles surface under the considered conditions. When particles are suspended in water, the presence of a C 1s peak at ~288.3 eV (the carbonate position CO_3^{2-}) supports the formation of $BaCO_3$ [27]. However, in agreement with the evolution of the peak percentages of the C 1s at ~290eV, and those of the O 1s

at 531.0 and 532.8 eV, the relative concentration of Ba-containing species at the particles surface decreases when solid content of the suspension increases. Contrarily, the presence of CuO increases drastically for 10 gl^{-1} suspension, according to the large ratio of the low BE of the O 1s peak (529.4 eV).

The determination of the atomic percentages of Y, Cu, Ba and C at the YBCO surface can help to explain the effect of solid content. Table 3 shows the atomic ratios of [Cu]/[Y], [Ba]/[Y], and [Ba]/[C] determined by XPS at the YBCO surface as a function of the solid loading. The [Cu]/[Y] atomic ratios for 0.1 and 1 gl^{-1} suspensions are close to that expected for the Y-123 phase, whereas the [Ba]/[Y] ratios for these suspensions verify the Ba dissolution revealed by the chemical analysis (Table 1).

Fig. 3: *Ba 3d peaks of treated YBCO powders under representative conditions compared with those of the as-received powders.*

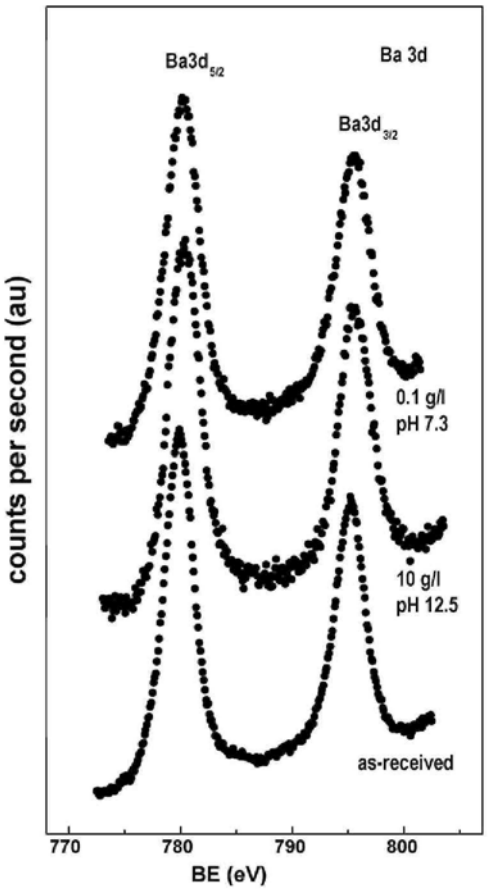

These data also evidence the strong increase of Cu concentration at the surface of the particles at the 10g l^{-1} suspension, which confirms the CuO precipitation determined by XRD and by XPS at the particles surface. The [Ba]/[Y] ratio supports the presence of Ba-containing species in concentrated suspensions, but in a lower amount than CuO under these conditions. Finally, the [Ba]/[C] ratio determines in all cases the presence of Ba species other than $BaCO_3$, suggesting the presence of hydrolysed species at the particles surface in agreement with the XPS spectra assignment.

It was tempting to see whether the Cu, Y and Ba percentages became distorted upon heating the samples under vacuum at temperatures of 240, 360 and 480 °C within the pretreatment chamber of the XPS spectrometer. YBCO powder of a 10g l^{-1} suspension was analysed for this purpose. For the samples pretreated at 240-480 °C, the binding energies of Cu 2p, Ba 3d and Y 3d levels remained unchanged, as observed in data shown in Table 4, but the concentration of these elements increased slightly up to a 9% at the highest temperature (480 °C). On the contrary, the O 1s component at 531 eV followed an opposite trend. This observation is consistent with a partial

decomposition of hydrolysed Ba species within the temperature range explored. Apparently, no change was observed in the intensity of the higher O 1s component associated to barium carbonate.

The analyses performed verify that YBCO dissolution takes place according to Eq. (1), suggesting the carbonation of the leached Ba under room conditions. The $BaCO_3$ and the CuO formation is more evident when the solid content increases. Similarly, the concentration of $Ba(II)_{aq}$ also increases with the powder concentration. However, the $Ba(II)_{aq}$, CuO and $BaCO_3$ concentrations in 10 g l^{-1} suspensions prepared at a prefixed pH between $7 \leq pH \leq 10$ decrease, indicating the partial reduction of the YBCO dissolution under these conditions. Furthermore, the high $Ba(II)_{aq}$ concentration in concentrated suspensions in agreement with the equilibrium diagrams suggests that Ba^{2+} and $Ba(OH)^{+}$ coexist in dissolution at pH>10, while XPS verifies the presence of Ba hydrolysed species at the particle surface, and the predominance of CuO over the Ba-containing species.

Table 3: *Cu/Y, Ba/Y and Ba/C ratios of the atomic percentages determined by XPS in YBaCuO samples vs. the suspension concentration and the pH in equilibrium.*

Concentration (gl^{-1})	pH in equilibrium	[Cu]/[Y]	[Ba]/[Y]	[Ba]/[C]
0.1	7.3	2.8	0.8	1.9
1	8.0	2.2	0.8	1.8
10	12.5	22.2	2.4	1.2

Table 4: *BE (eV) of core-levels of 10 gl^{-1}, pH 12, YBaCuO sample degassed in situ at various temperatures (numbers in parentheses are peak percentages).*

Sample	Cu $2p_{3/2}$	Ba $3d_{5/2}$	Y$3d_{5/2}$	O 1s	C 1s
	933.5	780.6	157.6	529.4 (50)	284.9 (49)
Without thermal				531.0(31)	288.8(22)
treatment				532.9(19)	290.5 (29)
				529.4 (63)	284.9 (57)
	933.4	780.4	157.7	531.1 (21)	288.7(18)
240 °C				532.8 (16)	290.4 (25)
				529.5 (66)	284.9 (64)
	933.5	780.5	157.6	531.2(19)	288.6(16)
360 °C				532.7 (15)	290.5 (20)
				529.5 (69)	284.9 (65)
	933.3	780.6	157.5	531.0(16)	288.7(15)
480 °C				532.8 (15)	290.3 (20)

3.2. Colloidal behaviour of the YBCO particles in aqueous suspension

The consequences of the increase of the solid concentration on the YBCO dissolution and the suspension pH were determined by the results described above. In this section, the pH evolution and the colloidal behaviour of the suspensions were determined under two different atmospheres (air and inert). The 0.1, 1 and 10g l^{-1} suspensions were sonicated for 2 min and homogenised by maintaining them stirring for 4 h in air (presence of CO_2) and under inert atmosphere (N_2 flow). The experimental values of pH are plotted in Fig. 4. The pH of the 0.1, 1 and 10g l^{-1} sonicated suspensions ($t = 0$) under open conditions are 7.5, 10.5 and 12, respectively. If the presence of CO_2 is avoided (i.e. nitrogen atmosphere), the pH ($t = 0$) are 9.3 and 10.5 in 0.1 and 1g l^{-1} suspensions, respectively.

A slight decrease of pH occurs for 0.1g l^{-1} suspension in air for the 30 first minutes of the homogenising time, achieving a constant value of about 7.3 after 2.5 h. For 1g l^{-1} suspension a larger pH decrease can be measured in air, from 10.5 to 8.0, before suspension achieves the equilibrium. The starting pH of 10g 1^{-1} suspension in air is nearly 12 and tends to increase toward 12.5 after 2.5 h, maintaining later this value. When decarbonated water and nitrogen flow are used for 0.1 gl^{-1} suspension, the pH slightly increases from 9.3 to 9.7 during 2.5 h, becoming constant for longer stirring times. The pH of 1 gl^{-1} suspension under these conditions maintains at 10.6 for 4 h. In all cases, suspensions pH maintains constant after 4 h stirring.

Fig. 4: *Evolution of pH with time in air and nitrogen atmosphere for 0.1, 1 and 10 gl^{-1} suspensions.*

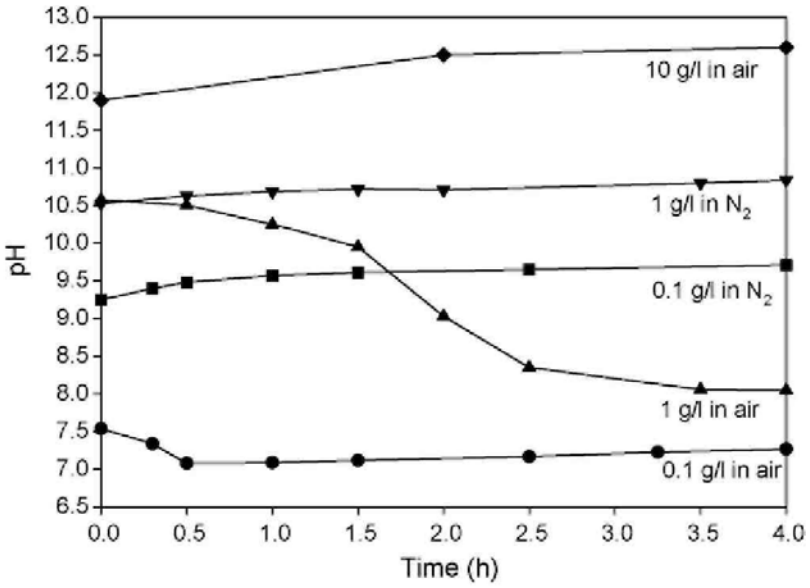

Plots in Fig. 4 demonstrate that the pH of YBCO aqueous suspensions varies with the experimental conditions (atmosphere and homogenising time) and the solid content. The ICP and XPS analyses of samples in equilibrium have revealed the selective dissolution of Ba^{2+}, and the presence of CuO, $BaCO_3$, and Ba hydrolysed species at the surface of the particle, especially at basic pH. Hence, the knowledge of the acid-base reactions of these species is necessary to study the evolution of the YBCO aqueous suspension. The main reactions in the system $Ba^{2+}/CO_2/H_2O$ are [14,16,17,19]:

$$Ba^{2+} + H_2CO_3 \rightarrow BaCO_3 + 2H^+ \quad (2)$$

$$Ba^{2+} + HCO_3^- \rightarrow BaCO_3 + H^+ \quad (3)$$

$$CO_{2aq} \leftrightarrow HCO_3^-;\ pK_a = 6.4 \quad (4)$$

$$HCO_3^- \leftrightarrow CO_3^{2-};\ pK_a = 10.3 \quad (5)$$

$$Ba^{2+} + OH^- \rightarrow Ba(OH)^+ \quad (6)$$

$$Ba^{2+} + 2OH^- \rightarrow Ba(OH)_2;\ pK_a = 2.2 \quad (7)$$

$$Ba(OH)_2 + CO_2 \rightarrow BaCO_3 + H_2O \quad (8)$$

As explained above, the Ba predominating species are determined by the pH and the concentration of $Ba(II)_{aq}$. In air, dissolved Ba^{2+} could react in a very basic suspension (pH>12) to form Ba $(OH)^+$ and/or $Ba(OH)_2$ (Eqs. (6) and (7)). Those species should react with atmospheric CO_2 leading to the formation of $BaCO_3$ (Eq. (8)). Similarly, dissolved Ba^{2+} can directly react with carbonates in acidic media to produce $BaCO_3$ (Eqs. (2) and (3)). A decrease of pH would be the main consequence, which is observed in the evolution of 0.1 and 1 gl^{-1} suspensions in air (Fig. 4). If there is no source of CO_2 (from either water or air), reactions (2), (3), and (8) cannot develop, and pH remains constant or tends to increase due to the continuous YBCO dissolution, as it occurs under nitrogen atmosphere (Fig. 4).

Low amount of YBCO results in a low quantity of dissolved Ba^{2+}, which quickly reacts with carbonates in open conditions to produce $BaCO_3$ (Eq. (8)), leading to an acid medium. In fact, the initial pH of 0.1 gl^{-1} suspensions is different for each condition, i.e. pH 7.5 in air and pH 9.3 under nitrogen flux in our system, suggesting a fast carbonation of leached Ba^{2+} during the suspension preparation in air. The effect of Ba^{2+} carbonation is more evident for the 1gl^{-1} suspension, which change its pH from 10.5 to 8.0 during the homogenisation time. The continuous acidification of the 0.1 and 1 gl^{-1} suspensions in air in Fig. 4 evidences the effects of Ba^{2+} carbonation, while it seems to have not effect over the 10gl^{-1} suspension pH. In this suspension, YBCO dissolution (Eq. (1)) governs the pH evolution.

Fig. 5: *Evolution of zeta potential with time in air and nitrogen atmosphere for 0.1, 1 and 10gl^{-1} suspensions.*

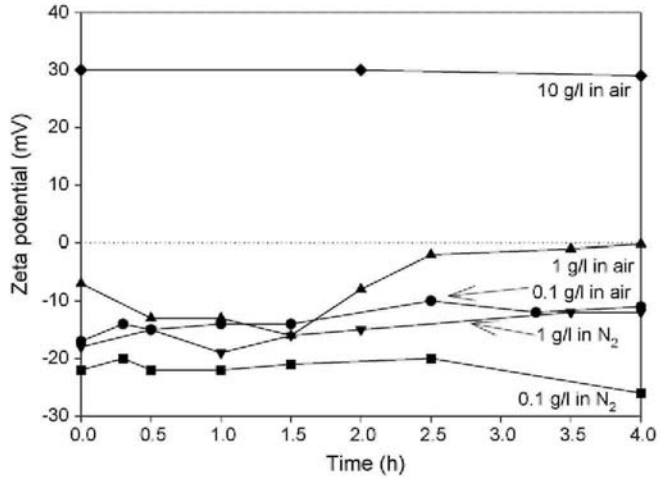

Fig. 5 shows the zeta potential evolution of the three suspensions measured at the same time as pH in Fig. 4. The 0.1 and 1 g l^{-1} suspensions show negative zeta potentials, while the 10 gl^{-1} suspension shows only positive values. When 0.1 gl^{-1} suspensions are maintained in open air, zeta potential changes to lower absolute values (from -16 to -12 mV). Contrarily, under inert atmosphere zeta potential tends to higher absolute value (from -20 to -26 mV). The 1 gl^{-1} suspension maintained in air shows very low zeta potential values when the suspension pH moves to 8. Zeta potentials of 1 gl^{-1} suspension in nitrogen atmosphere decrease very slightly from -18 to -12 mV. Finally, concentrated 10 g l^{-1} suspensions give a constant and positive value of 30 mV in air. Low concentrated suspensions (0.1 and 1 gl^{-1}) show a destabilisation tendency in air. Therefore, the amount of powder in the suspension and related reactions in water has a clear influence on the evolution of the surface charge of the particles.

A complementary experiment was performed to determine the effect of dilution on the surface of the YBCO particles. A suspension of 10gl^{-1} was prepared, after which it was diluted adding 2 ml/min of pure deionised water under the two considered atmospheres. Values of pH and zeta potential measured during dilution are plotted in Fig. 6. Under both atmospheres, dilution of the suspensions results in a decrease of the pH, similarly to the trend observed in Fig. 4. The zeta potential is positive for 10gl^{-1} suspensions and negative when solid concentration and pH decrease. The absolute zeta values are lower than those plotted in Fig. 5 for similar solid loadings. Dilution tests verify that the experimental conditions (atmosphere) determine the suspension pH, especially at the lower concentrations (0.1 and 1 gl^{-1}).

Fig. 6: *Effect of dilution on pH and zeta potential in air and nitrogen atmosphere.*

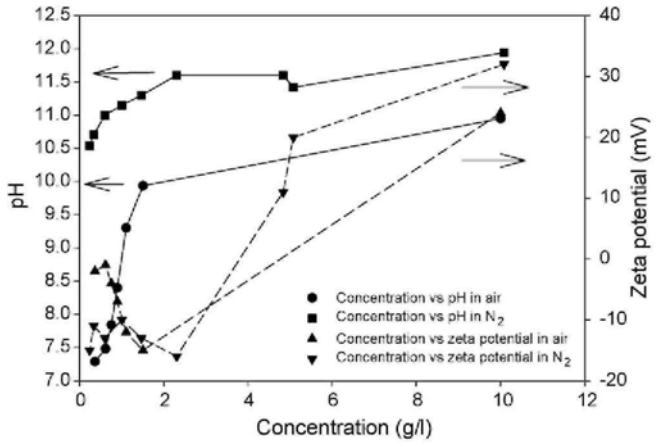

Fig. 7: *Evolution of zeta potential with pH for 0.1, 1 and 10 gl^{-1} YBCO suspensions homogenised during 48 h in air.*

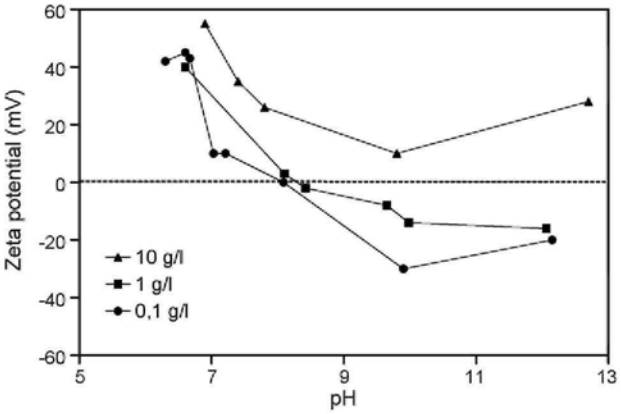

Two relevant facts related to the stability of the suspensions can be pointed out from these results. Assuming that the YBCO dissolution governs the suspension pH of the 10gl^{-1} suspension leading to a basic pH, either in air or inert conditions, the zeta potential is positive within the range of 24-34 mV (±5mV) pointing the stability of this suspension regardless of the $BaCO_3$. Hence, the effects of the carbonation of Ba^{2+} in air should be neglected in terms of suspension stability at this YBCO concentration.

Otherwise, a high concentration of $Ba(II)_{aq}$ remains dissolved after dilution of the 10gl^{-1} suspensions without effect on the charge of the YBCO particles in 0.1 and 1 gl^{-1} suspensions, apart from the increase of the ionic concentration which promotes the double layer thinning, and hence the low absolute zeta potential values measured during dilution, i.e. compare Figs. 5 and 6. Therefore, dilution tests determine that Ba^{2+} ions are not the only cause of the anomalous positive charge of particles in concentrated suspensions under basic conditions.

To preserve stability, suspension pH must be far away from the IEP. However, very few studies devoted to YBCO suspensions have reported the IEP value [22,23]. Fig. 7 shows the zeta potential of the YBCO suspensions prepared with different solid loadings: 0.1,1 and 10gl^{-1}. Zeta potential was in all cases measured after 48 h of homogenisation time. The first observation is the marked influence of the solid content on the IEP. For 0.1 gl^{-1}, the value of the IEP is about 8 so that particles are charged positively at pH<8 and negatively at pH>8. As already observed in previous studies [8-10] significant dissolution of YBCO is expected at weakly acidic pH (~6.5). The large concentration of counterions is responsible for the decrease of zeta potential, that is, the compression of the double layer. For more acidic pH strong dissolution occurs (Table 1). At highly basic pH, a slight decrease of zeta potential is also observed due to the increasing ionic concentration with KOH addition.

For 1 g l^{-1}, a similar behaviour is observed and the IEP value is around 8.3. Generally, absolute values of zeta potential at a basic pH (pH > IEP) are lower to those measured for 0.1 g l^{-1} suspension. The plot shows that the IEP slightly increases to basic pH when solid content increases from 0.1 to 1 gl^{-1}. However, no IEP could be detected for a solid concentration of 10gl^{-1}: the zeta potential remains positive all over the pH range.

Zeta potential values measured in equilibrium (after 48 h) at the natural pH of 0.1 and 1 gl^{-1} suspensions in air (pH 7.3 and 8.0, respectively in Fig. 7) did not correspond with those measured during suspensions evolution (Figs. 4 and 5) at a similar pH, while fit zeta potentials of the suspensions homogenised under inert atmosphere, avoiding Ba^{2+} carbonation, at pH 9.7 and 10.6, respectively (Figs. 4 and 5). Hence, the YBCO dissolution (Eq. (1)) and later cations activity, specifically that of Ba^{2+} carbonation (Eqs. (2) and (3)), promotes changes on the zeta potential leading to unstable systems for low concentrated suspensions. In those cases a large homogenising time to achieve the surface equilibrium could be needed.

Fig. 8: *Evolution of zeta potential of 0.1 g l^{-1} suspensions with concentration of the added cations.*

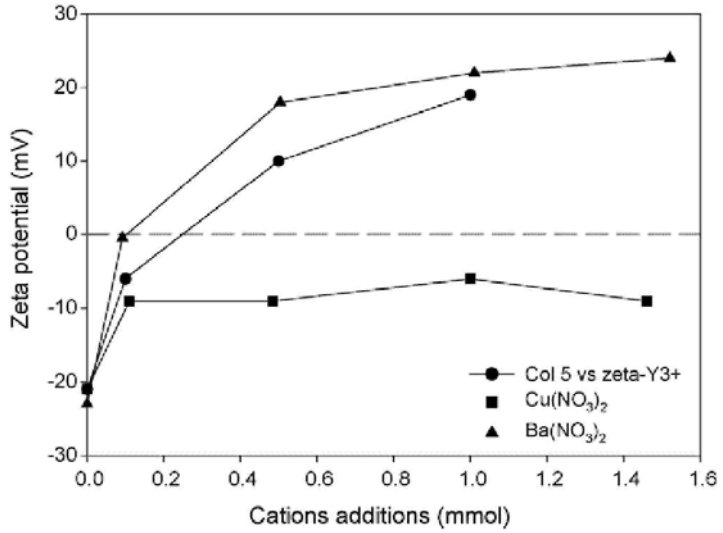

Fig. 9: *Evolution of zeta potential of 0.1 gl^{-1} suspensions with Ba^{2+} addition for different pH.*

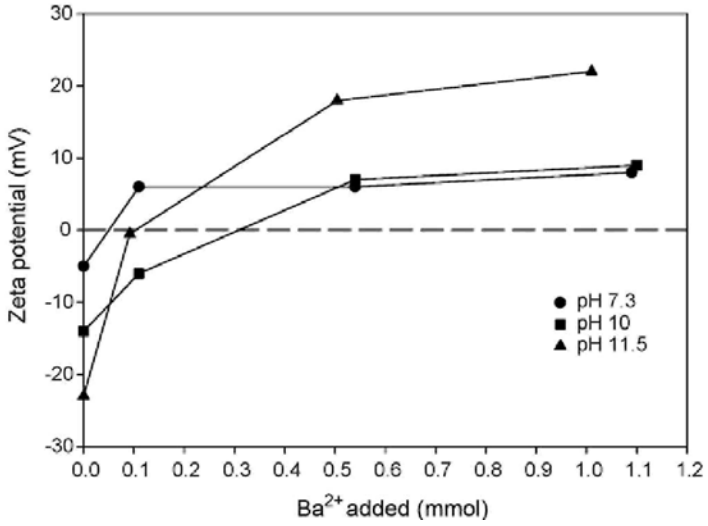

For the higher YBCO concentration tested, zeta potential remains positive in all range of pH and any IEP was determined. This behaviour has already been observed for $BaTiO_3$ suspensions with high solid concentration. Paik et al. [17] have observed a systematic shift of the IEP toward acidic pH with decreasing solid concentrations. The growth of a reactive Ba-depleted, TiO_2-enriched surface layer was proposed to explain the behaviour in acidic media. Bianco-Lopez et al. [14] have also observed the same behaviour for $BaTiO_3$ but the positive values at high solid contents were explained by the increase of Ba^{2+} concentration from $BaTiO_3$ or $BaCO_3$ impurity. According to these authors, a layer of $BaCO_3$ could be formed on the $BaTiO_3$ particles surface giving the surface behaviour of $BaCO_3$. Similarly, the YBCO surface would be covered by $BaCO_3$ after 48 h. Then the surface properties of particles should be dominated by the $BaCO_3$ ones.

To estimate the extent of the coverage of a $BaCO_3$ layer over the YBCO particles the zeta potential vs. pH of 0.1 gl^{-1} suspension of $BaCO_3$ in 10^{-2} M KC1 has been measured. The IEP of $BaCO_3$ is located around pH 9.5, about one pH unit above that of the YBCO powder. In fact, a positive zeta potential was also determined for 10g l^{-1} suspensions prepared under inert atmosphere in dilution tests (Fig. 6), hence $BaCO_3$ is not the responsible of the anomalous potential developed at the particles surface of concentrated suspensions. Similarly, different IEP of CuO were reported (from 4 to 8) [30,31], but they suggests that the presence of CuO at the particle surface should not be involved in the charging mechanism.

In order to estimate the incidence of dissolved cations on the zeta potential, nitrate salts of the three cations (Y/Ba/Cu) were added to $YBa_2Cu_3O_{7-x}$ suspensions (0.1 gl^{-1}) with a pH previously adjusted to 11.5. Fig. 8 shows that the increase of $Y(III)_{aq}$ and $Ba(II)_{aq}$ concentration is related to the change of the zeta potential from negative to positive. The plot verify that the increasing concentrations of Cu(II)aq have no influence on the zeta potential of the YBCO particles, due to the quick CuO precipitation at pH >8.

These analyses reveal that there is not $Y(III)_{aq}$ in the suspension (Table 1), but in the performed tests Y^{3+} precipitates easily as $Y(OH)_{3\downarrow}$ turning the suspension white. Above results confirm that only Ba species in solution should be the responsible forthe positive value of zeta potential at a basic pH when solid content increases.

Fig. 9 shows the influence of the concentration of $Ba(II)_{aq}$ and pH on the zeta potential. Three suspensions of 0.1 gl^{-1} were prepared and maintained at fixed pH of 7.3 (natural pH), 10 and 11.5. Before barium salt additions zeta potentials are negative for any pH. At pH 7.3, as expected by the IEP value of 8, zeta potential is near zero. The increase of $Ba(II)_{aq}$ concentration leads to a slightly positive zeta potential at any pH. The more basic is the pH, the faster is the zeta potential increase to higher positive values. In fact, when 1.5 mmol of Ba salt is added at pH 10, zeta potential is around +11 mV. When increasing the pH to 11.5 by addition of KOH, the zeta potential increases to +22 mV.

Studies related to the stability of soils components (such as clay and iron oxide minerals) reveal that the adsorption of charged species of the metals, present in natural or waste water systems, together with the precipitation of their hydroxides at the minerals surface is the dominant process in the surface charging in high alkaline suspensions [32,33]. The diagram of stability of Ba aqueous solutions plotted in Fig. 1 [25] shows that for pH > 10 both Ba^{2+} and $Ba(OH)^{+}$ coexist. ICP results confirm that $Ba(II)_{aq}$ concentration in 10gl^{-1} suspensions at pH 10 and 12 is over 0.1 mmol l^{-1} (Table 1), becoming $Ba(OH)^{+}$ the predominant species. Moreover, XPS verifies the presence of Ba hydrolysed species at the surface of dried powders previously dispersed in a 10 g l^{-1} suspension at its natural pH (12.5). According to Figs. 7 and 9, when Ba dissolution and pH conditions in the suspension lead to the formation of $BaOH^{+}$, whatever was the powder concentration (from 0.1 to 10 gl^{-1}) a high positive zeta potential value can be achieved under basic conditions. It occurs spontaneously for 10 g l^{-1} suspensions (Figs. 4-6), and when it is induced by the increase of the pH and the $Ba(II)_{aq}$ concentration for lower YBCO contents (Figs. 8 and 9). These results confirm that the mechanism of charging of the YBCO surfaces in aqueous suspensions strongly depends on the reactivity of the leached Ba^{2+} by incongruent dissolution of the YBCO. The concentration of dissolved Ba governs the behaviour of the particles surface in aqueous media at a basic pH.

In summary, the stability of YBCO suspensions depends on the formation and surface adsorption of $Ba(OH)^{+}$ species, i.e. basic pH and high Ba concentration. According to Eq. (1) and Fig. 2, the YBCO dissolution is partially inhibited under this conditions. So, the promotion of $Ba(OH)^{+}$ formation, and hence the development of the described charging mechanism of YBCO surfaces in water, open the possibility to shape this material through aqueous colloidal processes. However, a deep study should be still done to determine the effects of the proposed conditions on the structure-related properties of YBCO. Furthermore, those results can be extrapolated to other binary or ternary oxides structures composed by Ba or other cations with similar properties in aqueous media, such as Ca and/or Sr, which exhibit a similar incongruent dissolution of the related metal cation than YBCO, such as $BaTiO_3$ [14-17] or $BaZrO_3$.

4. Conclusions

The stabilisation mechanisms for YBCO particles in aqueous suspension were described. A route of particles stabilisation has been proposed that support the colloidal processing of the YBCO materials in aqueous media. To improve particles stabilisation, suspensions will be prepared at pH > 11 considering the addition of Ba salts, i.e. $Ba(NO_3)_2$, to avoid possible dissolution and promote the formation of Ba^{2+} hydrolysed species.

The surface chemistry of YBCO powders in aqueous media has been studied in depth. Results indicate the presence of $Ba(OH)^{+}$ in concentrated suspensions, which determines the evolution of the surface charge of the particles at basic pH. The presence of $Ba(OH)^{+}$ at the powder surface have been verified by the XPS degassing tests. Moreover, chemical and surface analyses verify the incongruent dissolution of Ba^{2+} in aqueous media, and its partial carbonation in air. XPS analysis also demonstrates that CuO precipitates at the surface of the particles for pH > 6. However, the formation of CuO has no effect in the charge evolution of YBCO in water.

The $BaCO_3$ formation governs the colloidal behaviour of low concentrated suspensions (0.1 and 1 g l^{-1}), while the YBCO dissolution determines that of 10 gl^{-1} suspensions. The XPS spectra suggest the presence of Ba carbonated species in the particles surface, but the tests developed under inert atmosphere verify that the presence of $BaCO_3$ is not responsible for the anomalous behaviour of YBCO in concentrated suspensions at basic pH, while it is the cause of the lack of stability of low concentrated suspensions during the homogenisation process.

Acknowledgements

The authors gratefully acknowledge financial support from the Belgian Science Policy (FNRS) under the Interuniversity Attraction Poles programme (INANOMAT - P6/17) and from the Spanish Science and Education Ministry (MEC) through Project MAT2006-01038, CCG08-CSICMAT-3811, CIT-420000-2008-2 and CIT-420000-2008-7.

References

[1] Y. Mao, T.J. Park, S.S. Wong, Chem. Commun. 46 (2005) 5721.

[2] O. Masala, R. Seshadri, Annu. Rev. Mater. Res. 34 (2004) 41.

[3] R. Moreno, Am. Ceram. Soc. Bull. 71 (1992) 1521.

[4] J. Su, V. Chintamaneni, M. Mukhopadhyay, IEEE Trans. Appl. Supercond. 17 (2007)3573.

[5] A.P .Finlayson,T. Mounganie, M.C.Cordero-Cabrera, B.A.Glowacki, Mater.Chem. Phys. 105 (2007) 99.

[6] J. Gazquez, F. Sandiumenge, M. Coll, A. Pomar, N. Mestres, T. Puig, X. Obradors, Y. Kihn, M.J. Casanove, C. Ballesteros, Chem. Mater. 18 (2006) 6211.

[7] J. Cwak, A. Ayral, V. Rouessac, L. Cot, J.C. Grenier, E.S. Jang, J.H. Choy, Mater. Chem. Phys. 84 (2004) 384.

[8] S.E.Trolier,S.D.Atkinson,PA. Fuierer,J.H.Adair,R.E. Newnham,Am.Ceram.Soc. Bull. 67 (1988) 759.

[9] K.G. Frase, E.G. Liniger, D.R. Clarke, Adv. Ceram. Mater. 2 (1987) 698.

[10] K· Komori, H. Kozuka, S. Sakka, J. Mater. Sci. 24 (1989) 1889.

[11] A. Barkatt, H. Hojaji, K.A. Michael, Adv. Ceram. Mater. 2 (1987) 701.

[12] M.F. Yan, R.L. Barns, H.M. O'Bryan, PIC Gallagher, R.C. Sherwood, S.Jin, Appl. Phys. Lett. 51 (1987) 532.

[13] R· Zhao, S. Myhra, Phys. C 230 (1994) 75.

[14] M.C. Bianco-Lopez, B. Rand, F.L Riley, J. Eur. Ceram. Soc. 17 (1997) 281.

[15] M.C. Bianco-Lopez, B. Rand, F.L Riley, J. Eur. Ceram. Soc. 17 (2000) 107.

[16] U. Paik, V.A. Hackley, J. Am. Ceram. Soc. 83 (2000) 2381.

[17] U. Paik, J.G. Yeo, M.H. Lee, V.A. Hackley, Y.G.Jung, Mater. Res. Bull. 37 (2002) 1623.

[18] C.W. Chiang, J.H. Jean, Mater. Chem. Phys. 80 (2003) 647.

[19] F· Boschini, A. Rulmont, R. Cloots, R. Moreno, J. Eur. Ceram. Soc. 25 (2005) 3195.

[20] G.L. Bhalla, S. Sharma, A. Malik, G.C. Trigunayat, Phys. C 284 (2003) 482.

[21] C.H. Lin, H.C.I. Kao, CM. Wang, Mater. Chem. Phys. 82 (2003) 435.

[22] A·Q Wang, T.R. Hart, Appl. Phys. Lett. 60 (1992) 1750.

[23] M.E. Labib, P.J. Zanzucchi, Inter. Phen. Biotech. Mater. Proc. (1988) 139.

[24] C.D. Wagner, L.E. Davis, M.V. Zeller, J.A. Taylor, R.H. Raymond, L.H. Gale, Surf. Interface Anal. 3 (1981) 211.

[25] F. Burriel, F. Lucen, S.Arribas,J. Henández, Química Analítica Cualitativa, Paran-info, Madrid, Spain, 1983.

[26] N. Casan-Pastor, P. Gomez-Romero, Phys. C 268 (1996) 268.

[27] J·H. Su, P.P. Joshi, V. Chintamaneni, S.M. Mukhopadhyay, Appl. Surf. Sci. 253 (2007) 4652.

[28] C.R. Brundle, D.E. Fowler, Surf. Sci. Rep. 19 (1993) 143.

[29] A· Gauzzi, H.J. Mathieu, J.H. James, B. Kellett, Vacuum 41 (1990) 870.

[30] J· Wang, Q. Zhang, F. Saito, Colloid Surf. A 202 (2007) 494.

[31] C. Li, M.H. Chang, Mater. Lett. 58 (2004) 3903.

[32] J· Lyklema, J. Colloid Interface Sci. 99 (1984) 109.

[33] M. Erdemoglu, M. Sarikaya, J. Colloid Interface Sci. 300 (2006) 795.